

Molecular Simulations Suggest Protein Salt Bridges Are Uniquely Suited to Life at High Temperatures

Andrew S. Thomas and Adrian H. Elcock*

Contribution from the Department of Biochemistry, University of Iowa,
51 Newton Road, Iowa City, Iowa 52242

Received October 21, 2003; E-mail: adrian-elcock@uiowa.edu

Abstract: A series of explicit solvent molecular dynamics simulations has been performed to investigate the temperature dependence of salt bridge interactions between two freely diffusing amino acids. The simulations, performed at 25, 50, 75, and 100 °C, allow a large number of distinct association and dissociation events to be directly observed, without the imposition of additional forces to drive association. Analysis of contact frequencies for atom pairs demonstrates that the number of salt bridge contacts between the two molecules is unaffected by temperature, whereas the numbers of hydrophobic and polar contacts are greatly diminished. A second, independent set of simulations—using rigid, prototypical molecule types—allows the differing temperature dependences of hydrophobic, polar, and salt bridge interactions to be unambiguously examined. In the prototype molecule simulations, the salt bridge interaction is found to substantially increase in stability at 100 °C relative to 25 °C. This difference in behavior between flexible amino acids and rigid prototype molecules is perhaps a direct manifestation of the effects of conformational entropy on association thermodynamics. Overall, the results demonstrate that salt bridge interactions are extremely resilient to temperature increases and, as such, are uniquely suited to promoting protein stability at high temperatures.

Introduction

The question of how proteins from hyperthermophilic organisms can maintain stability at much higher temperatures than those achieved by their orthologs from mesophilic organisms continues to attract attention. The availability of high-resolution structures (see, e.g., refs 1 and 2) has enabled comparative studies to be performed, and as a result, a number of factors have been suggested to be responsible for increased thermal stability; examples include improved packing in the hydrophobic core,³ shortening of flexible loops,⁴ and increased hydrogen bonding.⁵ Very recently, it has also been suggested that more basic characteristics of the protein fold may play a role.⁶ The most commonly cited feature, however, is an increased number of salt bridges^{7,8} and salt bridge networks distributed over the protein surface (for reviews, see, refs 9–11); in fact, it has been suggested that optimization of electrostatic interactions is a general determinant of enhanced thermostability.^{12–14} Interest-

ingly, in addition to direct structural evidence, a preference for charged residues is also evident at a genomic level: the frequencies of lysine, arginine, glutamate, and aspartate are all considerably higher in hyperthermophiles than in mesophiles.¹⁵

The preference for salt bridges in hyperthermostable proteins is intriguing given that the stability of proteins is more often associated with the burial of hydrophobic side chains than it is with formation of favorable electrostatic interactions. Site-directed mutagenesis studies of salt bridges in proteins have generally indicated that their contributions to stability are rather limited¹⁶—although it has been nicely demonstrated that substantial stability changes can be achieved by altering certain surface salt bridges.^{17,18} Rationalization of these latter works has benefited considerably from the availability of computational methods that provide accurate descriptions of electrostatic interactions in macromolecules.^{13,14,19–23} Several theoretical groups have concluded that while isolated salt bridges are generally of marginal stability,^{16,17} participation in salt bridge networks might have a powerful stabilizing effect.^{19–22}

- (1) Yip, K. S. P.; Stillman, T. J.; Britton, K. L.; Artymiuk, P. J.; Baker, P. J.; Sedelnikova, S. E.; Engel, P. C.; Pasquo, A.; Chiaraluce, R.; Consalvi, V.; Scandurra, R.; Rice, D. W. *Structure* **1995**, *3*, 1147–1158.
- (2) Hennig, M.; Darimont, B.; Sterner, R.; Kirschner, K.; Jansonius, J. N. *Structure* **1995**, *3*, 1295–1306.
- (3) Chan, M. K.; Mukund, S.; Kletzin, A.; Adams, M. W. W.; Rees, D. C. *Science* **1995**, *267*, 1463–1469.
- (4) Thompson, M. J.; Eisenberg, D. *J. Mol. Biol.* **1999**, *290*, 595–604.
- (5) Vogt, G.; Woell, S.; Argos, P. *J. Mol. Biol.* **1997**, *269*, 631–643.
- (6) England, J. L.; Shakhnovich, B. E.; Shakhnovich, E. I. *Proc. Natl. Acad. Sci. U. S. A.* **2003**, *100*, 8727–8731.
- (7) Perutz, M. F. *Science* **1978**, *201*, 1187–1191.
- (8) Fersht, A. R. *J. Mol. Biol.* **1972**, *64*, 497–509.
- (9) Szilágyi, A.; Závodszy, P. *Structure* **2000**, *8*, 493–504.
- (10) Kumar, S.; Nussinov, R. *Cell. Mol. Life Sci.* **2001**, *58*, 1216–1233.
- (11) Karshikoff, A.; Ladenstein, R. *Trends Biochem. Sci.* **2001**, *26*, 550–556.
- (12) Spassov, V. Z.; Karshikoff, A. D.; Ladenstein, R. *Protein Sci.* **1995**, *4*, 1516–1527.

- (13) Xiao, L.; Honig, B. *J. Mol. Biol.* **1999**, *289*, 1435–1444.
- (14) Dominy, B. N.; Perl, D.; Schmid, F. X.; Brooks, C. L., III. *J. Mol. Biol.* **2002**, *319*, 541–554.
- (15) Cambillau, C.; Claverie, J. M. *J. Biol. Chem.* **2000**, *275*, 32 383–32 386.
- (16) Strop, P.; Mayo, S. L. *Biochemistry* **2000**, *39*, 1251–1255.
- (17) Takano, K.; Tsuchimori, K.; Yamagata, Y.; Yutani, K. *Biochemistry* **2000**, *39*, 12 375–12 381.
- (18) Makhatazde, G. I.; Loladze, V. V.; Ermolenko, D. N.; Chen, X.; Thomas, S. T. *J. Mol. Biol.* **2003**, *327*, 1135–1148.
- (19) Hendsch, Z. X.; Tidor, B. *Protein Sci.* **1994**, *3*, 211–226.
- (20) Kumar, S.; Nussinov, R. *J. Mol. Biol.* **1999**, *293*, 1241–1255.
- (21) Kumar, S.; Ma, B.; Tsai, C.-J.; Nussinov, R. *Proteins* **2000**, *38*, 368–383.
- (22) Lounnas, V.; Wade, R. C. *Biochemistry* **1997**, *36*, 5402–5417.
- (23) Luo, R.; David, L.; Hung, H.; Devaney, J.; Gilson, M. K. *J. Phys. Chem. B* **1999**, *103*, 727–736.

Our own approach to the salt bridge/hyperthermostability issue has been to question whether there is anything intrinsic to salt bridge interactions that makes them more suited to promoting stability at high temperatures than other types of interactions. To this end, we previously focused on the role played by hydration effects and how this role might change at high temperatures. It is largely accepted that the association of salt bridge residues in water is less favorable than in the gas phase because the separated residues are more highly hydrated than their complex.¹⁹ In previous work we have argued that since this differential hydration effect becomes weaker as the temperature is increased, the salt bridge association should become stronger;²⁴ calculations based on a specially developed continuum solvation model²⁵ provided numerical support for this qualitative argument. Although this provides an appealing explanation for the increased predominance of salt bridge interactions in hyperthermophiles, the computational methods used to advance the argument have at least two limitations. First, our (and others') previous calculations of the thermodynamics of salt bridge interactions have made use of static models, so temperature-dependent changes in the conformational dynamics of the protein atoms have been ignored. Second, almost all previous thermodynamic studies have employed continuum solvent models to treat solvation effects. As powerful as they are, such methods are not a panacea, and it is quite possible that the molecular details of the solvent—which are omitted in such models—might be of critical importance, as was noted recently in simulations of β -hairpin folding.²⁶

An alternative to the use of continuum solvent methods is to include explicit solvent molecules in molecular dynamics (MD) simulations; this approach has the advantage that it allows conformational fluctuations within the salt bridge and fluctuations in its interactions with water to be modeled straightforwardly and simultaneously. Although explicit solvent MD simulations have been used to study the temperature-dependent dynamics of a small hyperthermostable protein (Sac7d),²⁷ the first work to directly compute thermodynamic information for amino acid salt bridge formation has been a recent report from Lazaridis and co-workers, who have computed potentials of mean force (PMF) for association at room temperature.²⁸ PMF computations provide significant insight, but their use of restraints to force association along user-defined pathways can in certain cases be a limitation. A solution to this problem has come from the recent realization that current computational resources, coupled with unforced explicit solvent MD simulations, can provide equilibrium association constants for small molecules in aqueous solution *without the need for the imposition of additional restraints*.^{29,30} This means that salt bridge interactions can now be investigated using molecular simulations that are as "natural" as possible: we can allow amino acids to freely diffuse and compute equilibrium constants simply by asking how often the molecules are associated with each other. In this way, temperature-dependent changes in solute–solute,

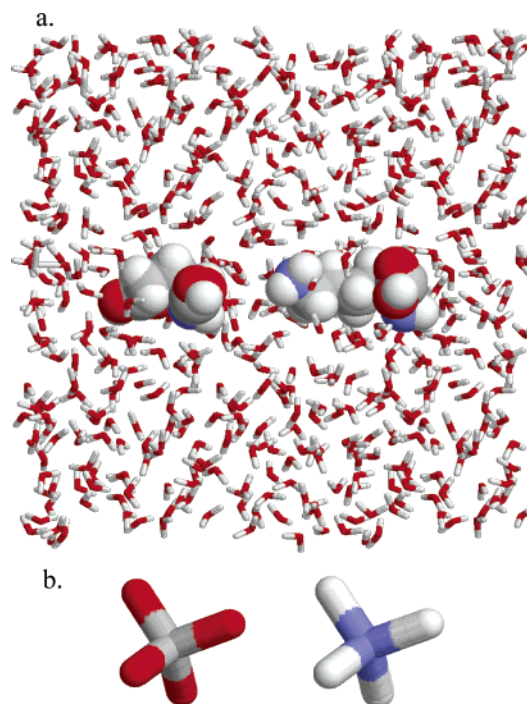


Figure 1. (a) Snapshot of the amino acid simulation system, showing the amino acid pair surrounded by SPC water molecules, (b) view of the artificial prototype molecules “CO₄” and “NH₄”.

and water–water interactions are all simultaneously captured, free of assumptions.

This manuscript describes the use of unforced MD simulations to study the association of two typical salt-bridging amino acids, lysine and glutamate, at four different temperatures (25, 50, 75, and 100 °C). We find that the frequency of salt bridge contacts formed by the charged side chains is insensitive to temperature in the range investigated, whereas the frequency of contacts formed between hydrophobic atoms and contacts formed between neutral polar atoms strongly decreases as temperature is increased. These trends are further examined in separate simulations employing prototypical molecules designed specifically to allow an unambiguous dissection of the behavior of hydrophobic–hydrophobic, polar–polar, and charge–charge interactions. Comparison of the two sets of simulations appears to provide an illustration of the role played by conformational entropy in molecular association.

Methods

Amino Acid Simulations. To test the temperature dependence of amino acid salt bridge formation, a simulation system containing a positively charged lysine and a negatively charged glutamate was modeled. The two molecules, initially separated by 12 Å, were placed at the center of a cubic box of length 30 Å, subject to periodic boundary conditions; the cube was filled with ~875 SPC water molecules,³¹ at a density ~1.0 g/mL. A view of the system at the beginning of the simulations is shown in Figure 1a. The system was energy-minimized with 100 steps of steepest descent and 1000 steps of conjugate gradient optimization. Independent MD simulations were then carried out at four different temperatures with the temperature controlled by the Nosé–Hoover method,^{32,33} and the pressure maintained at 1 atm

(24) Elcock, A. H. *J. Mol. Biol.* **1998**, *284*, 489–502.

(25) Elcock, A. H.; McCammon, J. A. *J. Phys. Chem. B* **1997**, *101*, 9624–9634.

(26) Zhou, R.; Berne, B. J. *Proc. Natl. Acad. Sci. U.S.A.* **2002**, *99*, 12 777–12 782.

(27) de Bakker, P. I. W.; Hünenberger, P. H.; McCammon, J. A. *J. Mol. Biol.* **1999**, *285*, 1811–1830.

(28) Masunov, A.; Lazaridis, T. *J. Am. Chem. Soc.* **2003**, *125*, 1722–1730.

(29) Yang, H.; Elcock, A. H. *J. Am. Chem. Soc.* **2003**, *125*, 13 968–13 969.

(30) Zhang, Y.; McCammon, J. A. *J. Chem. Phys.* **2003**, *118*, 1821–1827.

(31) Berendsen, H. J. C.; Postma, J. P. M.; van Gunsteren, W. F.; Hermans, J. In *Interaction Models for Water in Relation to Protein Hydration*; Pullman, B., Ed.; Reidel Publishing Company: Dordrecht, The Netherlands, 1981; p 331.

(32) Nosé, S. *J. Chem. Phys.* **1984**, *81*, 511–519.

using the Parrinello–Rahman method.³⁴ All covalent bonds were constrained with the LINCS algorithm,^{35,36} allowing a time step of 2 fs to be used in all simulations. A cutoff distance of 12.5 Å was used for short-range electrostatics and van der Waals interactions, but crucially, all electrostatic interactions beyond this distance were also computed using the particle-mesh Ewald (PME) method³⁷ with an interpolation order of 4. All simulations employed the GROMACS all atom force field,³⁸ with the termini of both amino acids modeled in uncharged states ($-\text{NH}_2$ and $-\text{COOH}$), in order (a) to make the simulations more representative of the situation in a protein and (b) to not complicate interpretation because of the presence of multiple interacting charged groups. For each temperature studied, three independent 100-ns trajectories were computed with the molecular simulation program GROMACS version 3.0;³⁸ structural snapshots were saved every 1 ps for subsequent analysis. A 100-ns amino acid simulation required approximately 25 days of CPU time when performed on a single Pentium 4 (2.5 GHz) processor.

To understand the effects of temperature on different types of atomic interactions, distance-based criteria were used to classify the contacts observed in the structural snapshots. Salt bridge contacts were defined by monitoring the distance between $\text{N}\zeta$ of lysine and $\text{C}\delta$ of glutamate. Polar–polar contacts were defined in terms of the distance between the N-terminal nitrogen of one molecule and the C-terminal carbon of the other molecule. Finally, hydrophobic–hydrophobic contacts were defined in terms of the minimum distance found between each possible pair of hydrophobic carbons in the two amino acids: this involved comparison of distances between $\text{C}\alpha$, $\text{C}\beta$, and $\text{C}\gamma$ of glutamate and $\text{C}\alpha$, $\text{C}\beta$, $\text{C}\gamma$, and $\text{C}\delta$ of lysine.

Prototype Molecule Simulations. To more cleanly dissect the temperature dependence of different types of interactions, a separate, independent series of simulations was performed monitoring the association of two artificial, prototype molecules; the two molecules, “ NH_4 ” and “ CO_4 ” (Figure 1b), are tetrahedral analogues of the NH_3^+ and COO^- groups found in the charged amino acids. Different partial charge sets were applied to these structural scaffolds to allow otherwise identical simulations to be performed of charge–charge, polar–polar, and hydrophobic–hydrophobic associations. For the charge–charge case, the partial charges assigned to “ CO_4 ” (C, +0.332e; O, –0.333e) summed to –1e; the charges assigned to “ NH_4 ” (N, –0.332e; H, +0.333e) summed to +1e. For polar–polar association, partial charges on both “ CO_4 ” (C, +1.332e; O, –0.333e) and “ NH_4 ” (N, –1.332e; H, +0.333e) summed to zero; for simulations of hydrophobic–hydrophobic association, all atoms were assigned partial charges of zero. MD simulations of these systems were performed using identical parameters to those used in the above amino acid simulations with the exception that a smaller box length was used (25 Å) and a short-range cutoff of 10 Å was applied to nonbonded interactions (long-range electrostatic interactions were again computed using the PME method). Association was defined in terms of the (intermolecular) distance between the central carbon and nitrogen atoms of the two molecules.

Computation of Prototype Molecule Association Free Energies. The intermolecular distances sampled in the structural snapshots were used to compute excess free energies of interaction for each distance in the following manner (see, e.g., ref 26). Expressing the distribution of intermolecular distances in histogram form allows the probability of the two molecules being found at a given separation distance (x) in the simulation ($P^x_{\text{simulation}}$) to be computed. To obtain the probability of finding the two molecules at the same separation purely by chance, a similar histogram was constructed from the results of 500 000 ran-

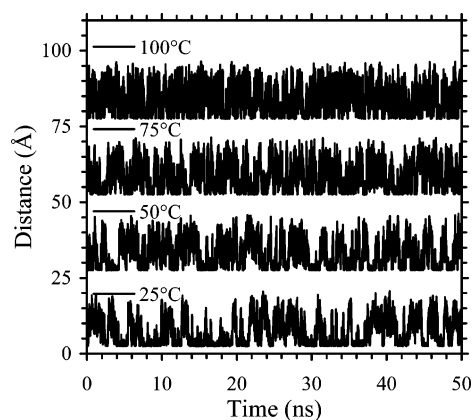


Figure 2. Plot of minimum distance between pairs of non-hydrogen atoms of the two molecules during MD simulations, with results for the higher temperatures offset by 25, 50, and 75 Å.

dom placements of the two molecules in the same simulation box ($P^x_{\text{random placement}}$). Given the two probabilities, the relative excess free energy at separation distance x (ΔG^x) can be calculated using

$$\Delta G^x = -RT \ln \left\{ \frac{P^x_{\text{simulation}}}{P^x_{\text{random placement}}} \right\} \quad (1)$$

where T is the temperature in Kelvin and R is the gas constant. Plots of these relative free energies were placed on an absolute scale by fitting to the analytical value of the Coulombic potential at the separation distance where sampling of configurations was maximal, ~ 13 Å, using appropriate values of the dielectric constant of water (see Results).

Results

Figure 2 shows how the minimum distance between non-hydrogen atoms of the lysine and glutamate molecules varies over half of a single 100-ns MD simulation performed at each of the temperatures 25, 50, 75, and 100 °C. Association events are identifiable as periods where the distance between the two molecules adopts a minimal value. Importantly, in each simulation many distinct association and dissociation events are observed: for example, at 25 °C more than 20 separate association events occur within 50 ns, and at higher temperatures the number of events increases substantially. Since the plots in Figure 2 show only one-sixth of the total simulation time for each condition (see Methods), it appears that the simulations have effectively explored the configurational space open to the two amino acids, providing confidence in the statistical significance of the results.

Support for this interpretation comes from examination of histograms of these minimum distance values (Figure 3): a gradual monotonic decrease in the total number of close contacts is observed as the temperature is increased. This decrease occurs despite the fact that the actual number of association events increases, because the *duration* of individual events is shorter at the higher temperatures (Figure 2). At first sight, the decrease in the overall extent of association implied by Figure 3 would seem to be inconsistent with the idea that salt bridge contacts might be resistant to temperature. However, it should be noted that the analysis at this point makes no distinction between different types of atomic contacts and therefore only demonstrates that the overall association of the two amino acids decreases at high temperatures. When we consider hydrophobic–hydrophobic, polar–polar, and charge–charge contacts separately, a more interesting picture emerges. Figure 4 shows the

(33) Hoover, W. G. *Phys. Rev. A* **1985**, *31*, 1695–1697.

(34) Parrinello, M.; Rahman, A. *J. Appl. Phys.* **1981**, *52*, 7182–7190.

(35) Miyamoto, S.; Kollman, P. A. *J. Comput. Chem.* **1992**, *13*, 952–962.

(36) Hess, B.; Bekker, H.; Berendsen, H. J. C.; Fraaije, J. G. E. M. *J. Comput. Chem.* **1997**, *18*, 1463–1472.

(37) Essman, U.; Perela, L.; Berkowitz, M. L.; Darden, T.; Lee, H.; Pedersen, L. G. *J. Chem. Phys.* **1995**, *103*, 8577–8592.

(38) Lindahl, E.; Hess, B.; van der Spoel, D. *J. Mol. Mod.* **2001**, *7*, 306–317.

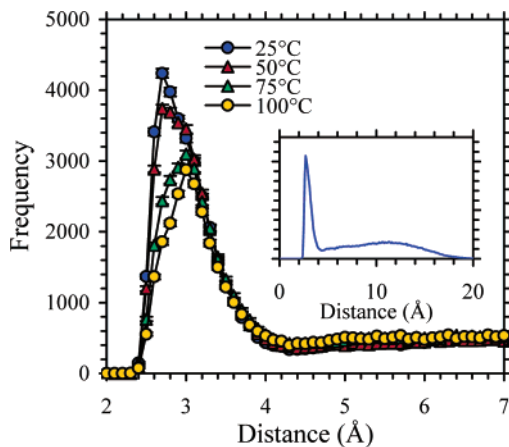


Figure 3. Histograms of minimum distance values between non-hydrogen atoms of the two molecules at the four temperatures studied. Inset shows the complete distribution obtained at 25 °C. Error bars for this and subsequent figures are standard deviations obtained from 1000 bootstrap samples of the simulation data.

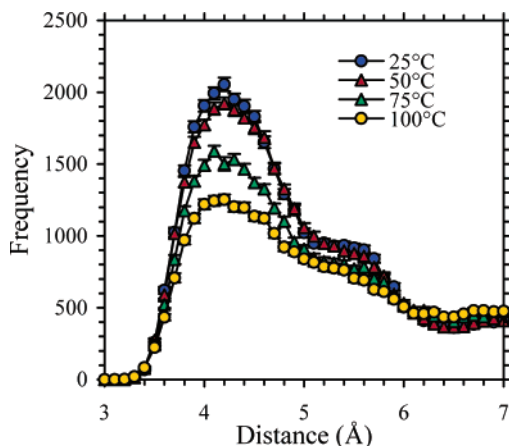


Figure 4. Histograms of minimum distances between hydrophobic atoms of the two molecules at the four temperatures studied.

histograms of hydrophobic–hydrophobic atom contacts (defined in Methods) at the four different temperatures investigated. These contacts constitute the majority of contacts seen in Figure 3 and show the same dramatic decrease as temperature increases, indicating not only that association has a significant hydrophobic component but also that its decrease at high temperatures coincides with a weakening of hydrophobic interactions. A similar weakening at high temperatures is displayed by interactions between the polar, neutral atoms of the amino and carboxyl termini (see Figure 5).

The decrease in hydrophobic–hydrophobic and polar–polar contacts with increasing temperature is in marked contrast to the behavior of salt bridge contacts (Figure 6). Using a reasonable definition of a salt bridge (i.e., that the distance between the carboxyl C and the amino N atoms be 4 Å or less), we can see that, far from decreasing with temperature, the number of such contacts remains more or less constant; this is a key result of the present work. Beyond 4 Å, a quite different behavior is observed, but this turns out only to be a consequence of the close proximity of hydrophobic and charged atoms in the amino acids: structural snapshots in which hydrophobic atoms are in direct contact with each other are naturally also likely to have their salt bridge atoms in relatively close contact, and vice versa. The apparent peaks at 5–6 Å in the salt bridge

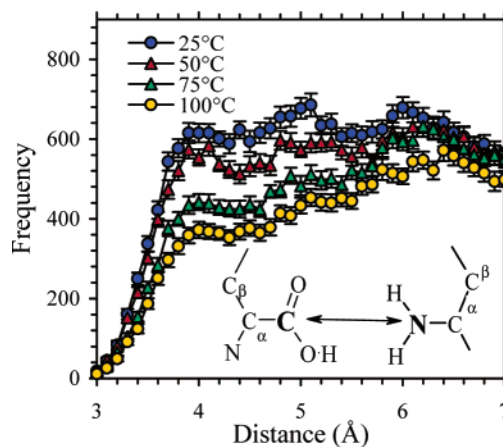


Figure 5. Histograms of distances between the C-terminal carbon of glutamate and N-terminal nitrogen of lysine at the four temperatures studied.

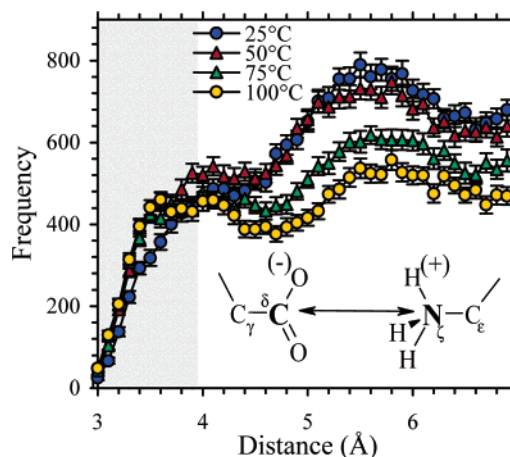


Figure 6. Histograms of distances between the salt bridge atoms at the four temperatures studied; the shaded region highlights contacts less than 4 Å in length.

contact distributions, then, are really only a reflection of the formation of *direct* contacts between hydrophobic atoms; this conclusion is supported by the observation that the 5–6 Å peaks in Figure 6 show the same dramatic temperature dependence seen in the hydrophobic contact distributions (see the 4 Å peaks of Figure 4). Implicit in the previous sentence, and obvious from inspection of Figure 6, is that the frequency of direct salt bridge contacts is much lower than that of hydrophobic contacts, suggesting that the charge–charge interactions contribute to, but do not dominate, the association of the two molecules, at least at low temperatures.

The fact that the histograms for the salt bridge contacts are strongly influenced by the hydrophobic–hydrophobic contacts makes unambiguously assessing the relative behaviors of the various types of interactions a formidable problem. Therefore, to simplify matters we performed an independent set of simulations investigating the association of structurally simpler, prototypical molecules (see Figure 1b and Methods). Pairs of these artificial molecules were separately simulated at 25 and 100 °C, with the intention of individually assessing the behavior of the following three kinds of interactions: (a) positive charge–negative charge; (b) neutral H-bond donor–neutral H-bond acceptor; (c) hydrophobic–hydrophobic. Intermolecular distance histograms were used to compute excess free energies of association as a function of the distance as described in Methods.

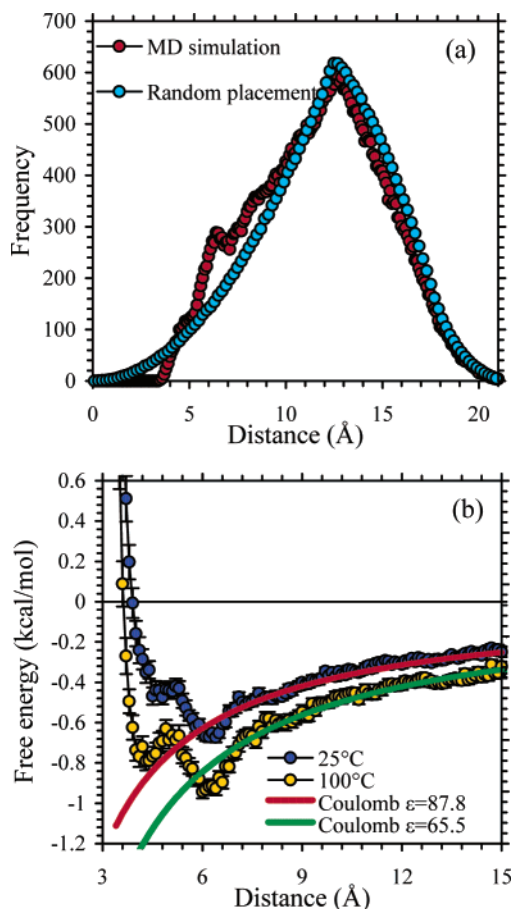


Figure 7. (a) Histograms of distances between carbon and nitrogen atoms of the charged prototype molecules at 25 °C. The red curve is the distribution obtained from the MD simulations; the blue curve is the distribution obtained from randomly placed structures. (b) Computed excess free energies of interaction for the charged prototype molecules.

The distance histograms at 25 °C, and the resulting computed free energy profiles, obtained from the charge–charge, polar–polar, and hydrophobic–hydrophobic simulations (all plotted on the same scale) are shown in Figures 7, 8, and 9, respectively (distance histograms at 100 °C are given in Figures S1–S3). The effectiveness of sampling in these simulations is especially evident in the hydrophobic and polar simulations: the histograms obtained from the MD simulations are in very close correspondence—at medium-long range—with those obtained from *randomly* placing the molecules in the same simulation box (see the close match of red and blue curves in both Figures 8a and 9a). The two charge–charge histograms (Figure 7a) do not show such a correspondence, but this is expected given the longer range nature of the electrostatic interactions.

Aside from the issue of sampling, several other more interesting findings emerge from inspection and comparison of these figures. First, in the free energy profile for charge–charge association (Figure 7b), a contact minimum at ~ 4.2 Å that forms only a shoulder to the curve at 25 °C becomes a distinct (local) minimum at 100 °C. Second, this same figure indicates that increasing the temperature makes the free energy of charge–charge association more favorable at *all* separation distances, not just those in which the salt bridge atoms are in direct contact. This includes solvent-separated “contacts” (see the minima at around 6 Å), therefore suggesting that long distance salt bridges, which may be missed in structural analyses, may also be

important for high-temperature stability; a suggestion to this effect was first made by Szilágyi and Závodszy.⁹ Third, for the charge–charge association, the computed free energies at longer distance (7–13 Å) are found to fit well to Coulomb’s law, allowing the dielectric constant of the solvent model to be easily determined. This approach, which has been attempted only once or twice before (see, e.g., refs 39 and 40) gives the dielectric constants of SPC water at 25 and 100 °C as being 87.8 and 65.5, respectively. While overestimating slightly the absolute values of the dielectric constant (the experimental values are 78.4 and 55.5 at 25 and 100 °C, respectively),⁴¹ the relative change from 25 to 100 °C is clearly in excellent agreement. Finally, with regard to the polar–polar and hydrophobic–hydrophobic associations (Figures 8b and 9b), two other points stand out. First, both show increased stability at high temperatures. This result concurs with other simulations aimed at understanding the temperature dependence of hydrophobic association,^{42–44} nevertheless, it stands in stark contrast to the behavior seen in the amino acid simulations, where a *decrease* in stability was observed (Figure 4). The possible reasons for this qualitative difference in behavior are discussed below. Second, the degree of stabilization of hydrophobic–hydrophobic association caused by the increase in temperature is smaller in magnitude than that observed for the charge–charge association (compare Figures 7b and 9b); the polar–polar results (Figure 8b) are intermediate between these two extremes but bear greater similarity to the hydrophobic–hydrophobic results.

Discussion

The simulations reported here indicate that favorable salt bridge interactions show a considerably greater degree of resistance to high temperature than either hydrophobic or polar interactions. As such, our results provide a clear conceptual basis to the engineering of salt bridges in efforts to develop thermostable proteins for industrial or scientific applications. Given that there have already been advances in engineering thermal stability by targeting electrostatic interactions (see, e.g., refs 17, 18, 45), knowledge of the *intrinsic* suitability of salt bridges for high temperatures should make such efforts even more tractable. It is worth noting of course that since our simulations do not consider more than two amino acids, our findings do not directly relate to the issue of networking of salt bridges as a means of stabilizing proteins. However, the primary conclusion from this work, that salt bridge interactions (even at long distance) are especially stabilized by high temperature, is consistent with, if not directly supportive of, the possible role of extended networks in hyperthermostable proteins.

As with all work based solely upon molecular simulations, it is important to note the potential limitations of the computational methods. Although explicit solvent MD simulations have the advantage that they describe all types of atomic interactions (solute–solute, solute–solvent, and solvent–solvent) on an

(39) Dang, L. X.; Pettitt, B. M. *J. Phys. Chem.* **1990**, *94*, 4303–4308.

(40) Del Buono, G. S.; Figueirido, F. E.; Levy, R. M. *Chem. Phys. Lett.* **1996**, *263*, 521–529.

(41) Lide, D. R. *CRC Handbook of Chemistry and Physics*, 83rd ed.; CRC Press Inc.: Boca Raton, FL, 2003.

(42) Lüdemann, S.; Schreiber, H.; Abseher, R.; Steinhauser, O. *J. Chem. Phys.* **1996**, *104*, 286–295.

(43) Shimizu, S.; Chan, H. S. *J. Chem. Phys.* **2000**, *113*, 4683–4700.

(44) Southall, N. T.; Dill, K. A. *Biophys. Chem.* **2002**, *101*, 295–307.

(45) Sanchez-Ruiz, J. M.; Makhatazde, G. I. *Trends Biotech.* **2001**, *19*, 132–135.

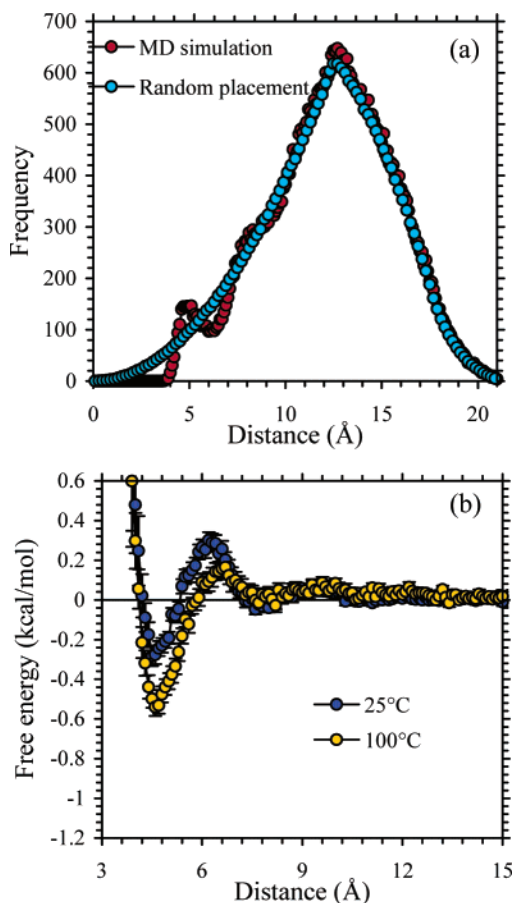


Figure 8. (a) Histograms of distances between carbon and nitrogen atoms of the polar prototype molecules at 25 °C. The red curve is the distribution from the MD simulations; the blue curve is the distribution from randomly placed structures. (b) Computed excess free energies of interaction for the polar prototype molecules.

equal basis, such simulations are not without drawbacks. For the purposes of discussion we divide these issues into the following three categories: (1) completeness of sampling, (2) accuracy of parameters, and (3) artifacts of the simulation methodology. In current applications of MD to biological systems, the first of these issues is usually an insurmountable problem: for example, simulations of even small proteins cannot currently be run for a sufficient length of time to adequately sample all their accessible conformations. In fact, problems with sampling have been one of the major motivations for the use of continuum solvent methods in computing salt bridge interactions.^{19–25} However, based on four lines of evidence we can be confident that a rather complete view of the association behavior has been attained in these explicit solvent simulations. First, as Figure 2 makes clear, for each temperature studied, we observe a large number of independent association and dissociation events. Second, in all cases, the histograms of the atomic contact distances show smooth distributions without any obvious discontinuities. Third, when the distributions obtained at different temperatures are compared, a smooth, gradual change in behavior is observed. Finally, and perhaps most compellingly, there is an extremely close fit, at medium-long range, between the intermolecular distance distributions obtained from the polar and hydrophobic prototype MD simulations and the corresponding distributions calculated by exhaustive, random placement of the two molecules into the simulation system at

both 25 and 100 °C (see Figures 8a and 9a and Figures S2 and S3 in the supporting information).

In much the same way that we expect inadequate sampling not to be an issue here, we expect that the second common issue associated with MD, questions over the accuracy of the molecular force field, will also be less of a concern. This is not to say that the force field in use has been demonstrated to be of quantitative accuracy; it has not. It is rather that the major focus of the present work is on the temperature dependence of association rather than its absolute magnitude. Because of this, all that we require is that the relative effects of temperature on solute–solute, solute–water, and water–water interactions be adequately reproduced. It is difficult to unambiguously establish whether this is the case for the first two types of interactions, but as reflected in the computed temperature dependence of the SPC water dielectric constant (which is in excellent agreement with experiment) the electrostatic screening properties of the solvent–solvent interaction are adequately described by the model used in the simulations. Correctly reproducing all other thermodynamic properties of water, such as the temperature dependence of its density, is difficult for simple three-site water models.⁴⁶ The SPC model has been shown previously to be comparable to TIP3P and TIP4P water models in predicting a ~7% decrease in density between 25 and 100 °C.⁴⁷ In our prototype salt bridge simulations we find an identical 7% drop in system density (data not shown), but it should be noted that this does not match the experimental drop of 3.8%.⁴¹ Although this is a clear discrepancy, we expect it to be less critical to the modeling of molecular associations than the proper modeling of water’s dielectric properties.

The final simulation issue to address concerns the possible role played by simulation artifacts, by which we mean problems unintentionally introduced by the procedures employed to accelerate the computations. Foremost among the issues to be concerned with is the way in which electrostatic interactions are treated in the simulations; this is especially important given the less than glorious past of MD simulations in modeling interactions between charged molecules. Although our simulations employ what is currently considered to be the "state of the art" method for dealing with electrostatic interactions (the PME method), it is important to note that this method is not without its own drawbacks: for example, the use of PME has been suggested to affect ion interactions⁴⁸ and to artificially stabilize the α -helical form of an octapeptide.⁴⁹ As a separate, explicit test of PME effects we investigated the temperature dependence of association for the charged amino acid pair in a continuous dielectric medium with (a) the PME method and (b) electrostatic interactions truncated at 12.5 Å (see Supporting Information); essentially identical results were obtained regardless of which method was used to compute the electrostatic interactions (see Figures S4–S7 in the supporting information). Short of repeating all our explicit solvent simulations with other less generally accepted schemes for computing electrostatic interactions, we are reasonably confident that the results obtained

(46) Mahoney, W. M.; Jorgensen, W. L. *J. Chem. Phys.* **2000**, *112*, 8910–8922.

(47) Jorgensen, W. L.; Jensen, C. *J. Comput. Chem.* **1998**, *19*, 1179–1186.

(48) Hünenberger, P. H.; McCammon, J. A. *J. Chem. Phys.* **1999**, *110*, 1856–1872.

(49) Weber, W.; Hünenberger, P. H.; McCammon, J. A. *J. Phys. Chem. B* **2000**, *104*, 3668–3675.

are not a consequence of artifacts introduced by the PME method.

Even though our simulations consider interactions between only two amino acids, it is clear that there are a variety of factors that are at play: the lysine and glutamate molecules both introduce hydrophobic interactions in addition to electrostatic interactions, and deciding the extent to which the observed behavior is caused by the different types of interactions is not easy. Here we have sidestepped this problem by exploiting a seldom-used advantage of molecular simulations: their ability to simulate the behavior of artificial molecules. The advantage of such simulations is that they provide as unambiguous a view as possible of the kinds of contributions expected to be made by different types of interactions. The disadvantage of course is that they are not capable of being subjected to direct experimental testing, even though echoes of their behavior may be observed in "real" molecules (e.g., amino acids). Because of this, the power of these prototype simulations is most keenly felt when used to illuminate behavior observed in accompanying, structurally realistic simulations.

The prototype simulations reported here provide two striking illustrations of the utility of this kind of approach. The first was expected: the greater thermal stability of the artificial salt bridge interaction relative to the corresponding hydrophobic and polar interactions (Figures 7–9) was consistent with the behavior already observed in the amino acid simulations (Figures 4–6). The second was unexpected: in the case of the amino acids, the frequency of hydrophobic–hydrophobic contacts was found to *decrease* dramatically with temperature (Figure 4), whereas in the case of the hydrophobic prototypes, the frequency of contacts actually *increases*, so that their free energy of association became more favorable (Figure 9b). This result is intriguing and potentially important. Although properly establishing its causes will require further work, a reasonable current hypothesis is that it is a direct manifestation of the effects of conformational entropy loss upon association. The prototype molecules, being effectively spherical in shape and rigid, undergo only a very limited decrease in their degrees of freedom when they associate. The same cannot be said of the amino acids: both lysine and glutamate possess long flexible side chains and it is possible that a considerable decrease in their conformational freedom accompanies association. If this is indeed the cause of the different temperature dependencies, then we may eventually find interesting differences in association of residues that contain less flexible side chains (e.g., aspartate).

In closing, it is worth noting that the simulations reported here raise a number of points in addition to their implications for the thermal stability of proteins. First and most importantly, they demonstrate the feasibility of using *straightforward* MD simulations to compute the thermodynamics of association of small molecules in aqueous solution. This, together with other results that we have obtained for purely hydrophobic amino acids²⁹ (see also ref 30), suggests that it should now be possible to directly parametrize molecular force fields so that they are

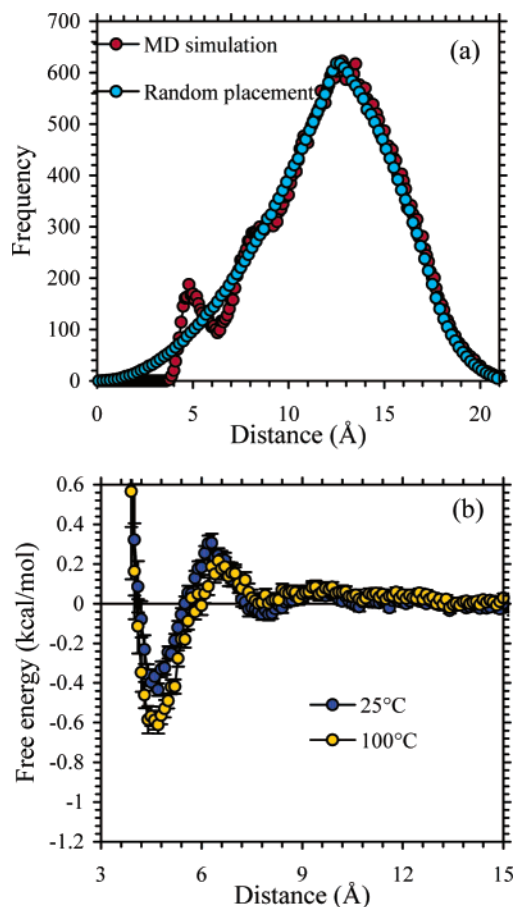


Figure 9. (a) Histograms of distances between carbon and nitrogen atoms of the hydrophobic prototype molecules at 25 °C. The red curve is the distribution from the MD simulations; the blue curve is the distribution from randomly placed structures. (b) Computed excess free energies of interaction for the hydrophobic prototype molecules.

consistent with experimental aqueous phase association data. Second, the interdependence of hydrophobic, polar, and charged interactions within single amino acid molecules demonstrates the complexities that will be commonly encountered in analyzing even the simplest residue–residue interactions. Finally, the use of prototypical molecule types, in conjunction with analogous simulations of structurally realistic molecules, provides a powerful means of dissecting individual contributions to otherwise complex behavior.

Acknowledgment. We are grateful to Tamara Frembgen Kesner for critical reading of the manuscript. This work was supported in part by the Irene Wells Medical Research Fund administered by the University of Iowa.

Supporting Information Available: Intermolecular distance histograms for prototype molecule simulations at 100 °C and results of stochastic dynamics simulations (PDF). This material is available free of charge via the Internet at <http://pubs.acs.org>.

JA039159C